FLUID FILLED CONTAINMENTS IMPACT BY A HIGH VELOCITY BULLET

Smirnova M.N.1,2, Kondrat'ev K.A.1

1Moscow M.V. Lomonosov State University, Moscow 119899, Russia
2 Saint Petersburg State Polytechnical University, 29 Politechnicheskaya Str., 195251 St. Petersburg Russia

Abstract: High velocity fragment or bullet interaction with thin walled fluid-filled containment is investigated. Fragment subsonic motion in compressible fluid was studied being the function of the depth of perforation under the water level in case the containment was partially filled with water and partially with gas having a distinct fluid-gas interface. Approximation formulas were developed making it possible to simulate resistance and drag forces being functions of governing parameters. The developed models were validated by comparing theoretical data with results of experiments. The obtained solutions are applicable for developing concepts for effective shield design protecting from high velocity fragments.

Keywords : fragment, impact, crater, fluid-filled containment, resistance force, perforation.

INTRODUCTION

Capturing high velocity impact fragments is an acute problem for protecting Space vehicles from different elements of Space debris [1-3], protecting aircrafts against accidental explosions of terroristic nature [4, 5]. Orbital debris environment is a serious hazard to Space missions nowadays. Collision with a debris metallic particle of 1 cm radius is energetically equivalent to a collision with half a ton mass car moving at a speed 100 km per hour. [6-9]. The problem of spacecrafts shielding from small particles could be solved protecting them by fluid-filled containments, which consume the impact energy and redistribute momentum on a wider area of protected wall [9-11].

The present paper is aimed at studying dynamics of impactor deceleration after wall perforation of the fluid filled containment. The problem will be studied being the function of the depth of perforation under the water level in case the containment is partially filled with water and partially filled with gas having a distinct fluid-gas interface. The models will be verified against results of experiments.

MODEL FOR PARTICLE INTERACTION WITH FLUID-FILLED CONTAINMENT

Most of spacecrafts contain pressurized gas-filled or fluid-filled vessels as structural elements. Fragmentation of a gas-filled or fluid-filled containment in hypervelocity collision has definite peculiarities and differs from trivial perforations of walls [1]. The present paper will describe the model for the fragment impact on a rather thin-walled containment, which could be filled in with gas, liquid, or both liquid and gas phases having a distinct phase interface. Ground-based experimental investigations described in [12] were performed, in particular, for aluminum cylindrical containments placed vertically, diameter 70 mm, wall thickness 0.1 mm, aluminum impactor $D = 5.4$ mm in diameter and length $L = (0.56 \div 1.0)D$, impact velocity ranging 2.7 – 3.0 km/s. Experiments performed by ourselves used the impactor mass 0.2 g accelerated up to 2.0 km/s. We used gas filled containments, fluid filled containments and partially filled with fluid, partially with gas. The scheme of experiments is shown in Fig. 1. In case of distinct fluid-gas interface the fragment perforated the wall at a different depth under the water level, which demonstrated different scenario of containment breakup.

Experiments showed, that in case impact took place above the liquid level the results were the same as for the gas filled containment: perforation of the front and rear walls. In case impactor collided the containment below the liquid level, catastrophic damage of the front or rear walls, or both could take place associated with fractures growth from the perforation zone in all directions and opening the walls of the containment outside as if being the result of intense internal loading. Fig. 2 shows containments

with front (perforated) wall broken, while the rear wall is not damaged.

Here we'll provide theoretical background for the observed phenomenon.

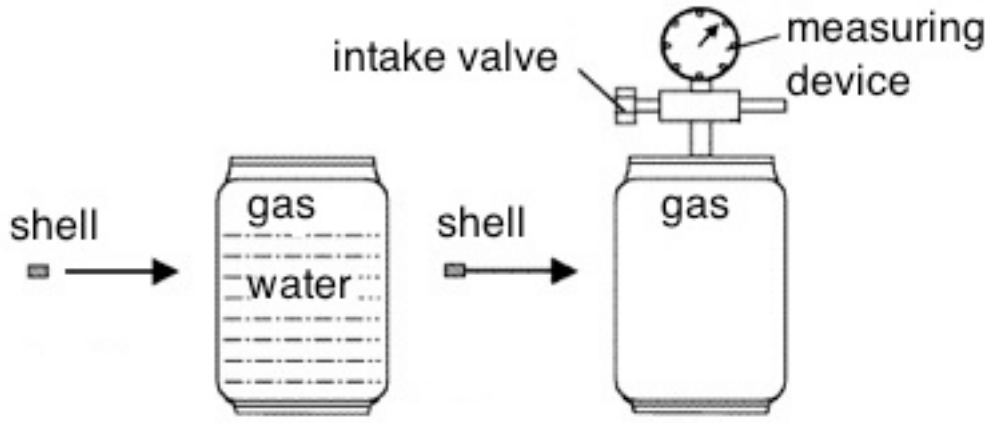

Fig.1. Experimental setup.

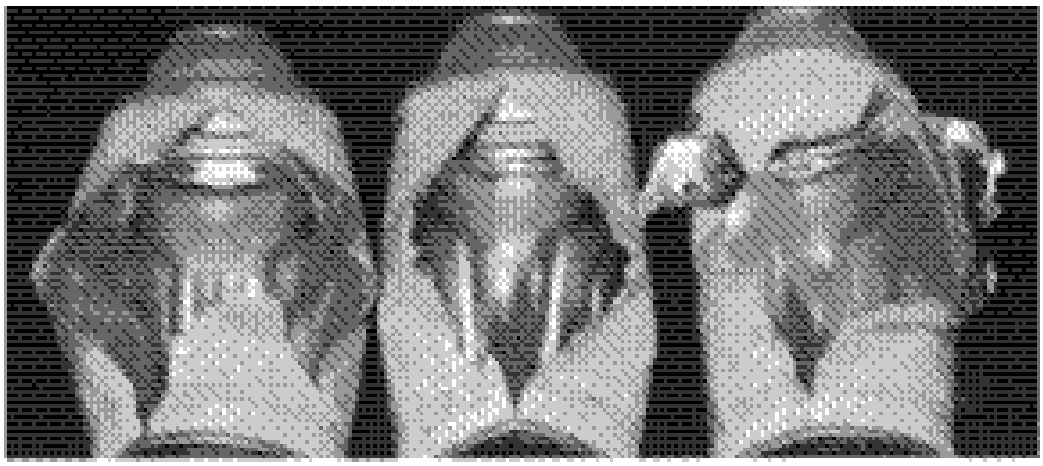

Fig. 2. Front view of fluid filled containments subjected to front impact.

Fragmentation of a gas-filled or fluid-filled containment in high velocity collision has several characteristic stages. The first stage is perforation of the wall in the collision zone and fragments penetration inside the containment. Formation of cracks (and petals) in the collision zone do not usually bring to a breakup of the containment at the present stage. The penetrating fragments form a shock wave in the media, filling the containment (Fig.3).

The fragments slow down very rapidly due to the drag forces. The deceleration for fragments is proportional to $1/r_0$ and grows up with the decrease of a characteristic size r_0. The velocity decrease is exponential and could be estimated by formula:

$$v_{rel} = v_{rel}^0 \exp(-\frac{3}{8} C_d \frac{\rho}{\rho_c} \frac{x}{r_0}), \qquad (1)$$

where C_d is drag coefficient, ρ_c, ρ - density of fragment and gas respectively, r_0 - radius of fragment.

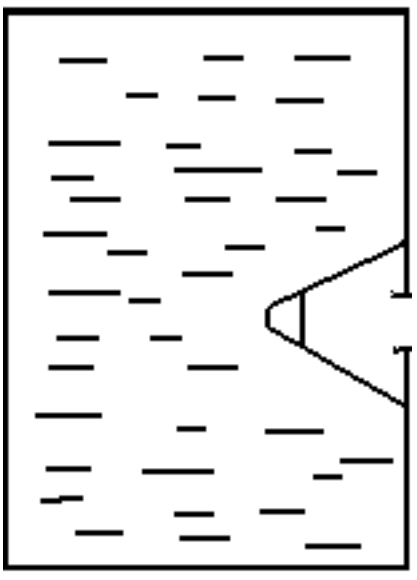

Fig.3. Schematic picture for fluid-filled containment perforation.

It is seen from (1) that on decreasing fragment size the slowing down distance also decreases. On slowing down the fragment conversion of its kinetic energy into the internal energy of the surrounding gas (or fluid) takes place. The rapid increase of the density of energy in a small volume inside the containment is similar to that for the local explosion. The energy release gives birth to diverging blast waves inside the containment that reflects from the walls thus producing non-uniform loading. The concentrated energy release causes blast waves of high intensity. Thus the wall being more close to the blast point exercises higher loading. The breakup of the wall causes the pressure drop and the rarefaction waves, which go inside the containment, overtaking the blast wave and lowering down its intensity [13 – 15]. Thus the far wall will be much less loaded.

As it is seen from formula (1) the rate of deceleration depends on density ratio. The less is the fluid density, the slower is deceleration, and the weaker is the shock wave formed inside containment. Due to that reason increase of overall initial pressure brings to formation of stronger shock waves and increase of the damage level. Penetration of fragment deep below the liquid level also brings to its faster deceleration due to much higher density ratio as compared to deceleration in gas. However, overall drag coefficient is dependent on the depth of fragment motion below the liquid-gas interface, because gas is highly compressible as compared with liquid, which permits fluid separation from the fragment thus reducing the drag on approaching the free surface [16, 17].

MATHEMATICAL STATEMENT FOR THE PROBLEM OF THIN FRAGMENT MOTION UNDER FREE SURFACE

The two-dimensional problem of fluid streaming thin fragment motion with formation of infinite (Fig. 4) or final length (Fig.5) cavity behind it velocity being parallel to free surface is regarded under the assumption of flow separation from the upper or lower surface of the fragment. In case of final cavity formation it is closed at some distance S from the fragment. Pressure on free surface is assumed equal to ambient pressure. Pressure in the cavity is assumed equal to the value of vapor saturation pressure depending on the constant of cavitation. Fluid is assumed to be ideal, depth – infinite, mass forces – negligibly small, flow field – plane.

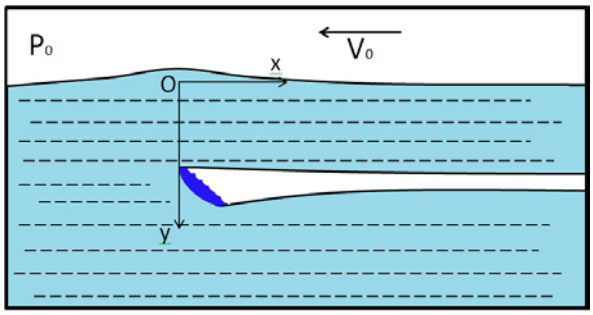

Fig.4. Formation of infinite cavity behind the fragment.

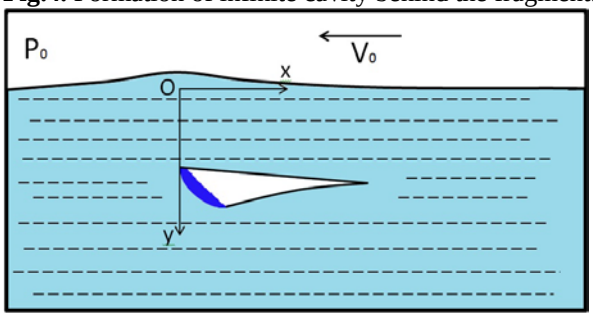

Fig. 5. Formation of final length cavity behind the fragment.

Velocity field in fluid is assumed to be potential

$$\vec{V} = \vec{V}_0 + grad\ \varphi,$$

fluid will be regarded as linear compressible

$$P = P_0 + a^2(\rho - \rho_0),\ a^2 = \left(\frac{dP}{d\rho}\right)_{\rho_0}, \quad (2)$$

$$P=P(\rho) \rightarrow dP = \left(\frac{dP}{d\rho}\right)_{\rho_0} d\rho,$$

where $\varphi(x,y,t)-$ disturbance velocity potential, $P, \rho-$ fluid pressure and density, P_0, ρ_0- pressure and density in quiescent fluid, $a-$ sonic velocity.

Fluid flow satisfies continuity equation

$$\frac{d\rho}{dt} + \rho\ div\,\vec{V} = 0, \quad (3)$$

pressure is determined by Cauchy-Lagrange integral

$$\frac{\partial\varphi}{\partial t} + \frac{(grad\ \varphi)^2}{2} + \int\frac{dP}{\rho} = c(t). \quad (4)$$

Flow induced variations of density and velocity are considered small values.

$$\rho'/\rho = (\rho - \rho_0)/\rho \ll 1;$$
$$V_x/V_0 \ll 1; V_y/V_0 \ll 1,$$

where V_x, V_y- disturbance velocity components.

Then it follows from continuity equation (3), integral (4) and relationship (2) neglecting small values of the orders higher than one, flow potential φ under the condition of steady-state flow satisfies the equation

$$V_0^2 \frac{\partial^2 \varphi}{\partial x^2} = a^2 \left(\frac{\partial^2 \varphi}{\partial x^2} + \frac{\partial^2 \varphi}{\partial y^2} \right), \qquad (5)$$

and fluid pressure is determined

$$P - P_0 = \rho_0 V_0 \frac{\partial \varphi}{\partial x}. \qquad (6)$$

Boundary conditions should be satisfied on the free surfaces, on the fragment surface contacting fluid and in the cavity. On the free surface and in the cavity constant pressure is assumed, on the fluid-fragment contact streaming condition of the equality of normal velocity component.

The obstacle being thin and inclination angle being small all disturbances could be considered small, and boundary conditions take the form

$$y = 0, \quad P - P_0 = 0;$$

$$y = h^+, 0 < x < L \quad V_y = \frac{\partial \varphi}{\partial y} = V_0 \cdot \sin\theta \qquad (7)$$

1. $y = h^-, 0 < x; \quad y = h^+, L < x \quad P - P_0 = 0$
2. $y = h^-, L < x; \quad y = h^+, 0 < x \quad P - P_0 = 0$
3. $$y = h^-, 0 < x < S \quad P - P_0 = -\Delta P \quad \Delta P = C_{\kappa a в.\min} \frac{\rho_0 V_0^2}{2}$$
$$y = h^+, L < x < S \quad P - P_0 = -\Delta P$$
$$y = h^{\pm}, S < x \quad V_x = 0.$$

Substituting in (7) dynamical equation (6) boundary conditions look as follows

$$y = 0, \quad \frac{\partial \varphi}{\partial x} = 0;$$

$$y = h^+, 0 < x < L \quad \frac{\partial \varphi}{\partial y} = V_0 \cdot \sin\theta;$$

1. $y = h^-, 0 < x; \quad y = h^+, L < x \quad \frac{\partial \varphi}{\partial x} = 0$ (8)
2. $y = h^-, L < x; \quad y = h^+, 0 < x \quad \frac{\partial \varphi}{\partial x} = 0$
3. $$y = h^-, 0 < x < S \quad \frac{\partial \varphi}{\partial x} = -\frac{\Delta P}{\rho_0 V_0}$$
$$y = h^+, L < x < S \quad \frac{\partial \varphi}{\partial x} = -\frac{\Delta P}{\rho_0 V_0}$$
$$y = h^{\pm}, S < x \quad \frac{\partial \varphi}{\partial x} = 0.$$

Thus equation (5) with boundary conditions (8) present a closed form statement of the problem.

SOLUTION FOR THIN FRAGMENT PENETRATION IN COMPRESSIBLE FLUID

We assume the flow to be subsonic. Then on introducing dimensionless parameter $\alpha = \sqrt{1 - M^2}$, where $M = V_0 / a -$ Mach number and dimensionless functions and variables

$$\varphi^* = \frac{\pi \varphi}{ah}; \; p^* = \frac{P - P_0}{\rho_0 a^2}; \; l = \frac{\pi L}{\alpha h}; \quad s = \frac{\pi S}{\alpha h};$$

$$x^* = \frac{\pi x}{\alpha h}; \quad y^* = \frac{\pi y}{h}, \qquad (9)$$

equations and boundary conditions take the form

$$\frac{\partial^2 \varphi^*}{\partial x^{*2}} + \frac{\partial^2 \varphi^*}{\partial y^{*2}} = 0, \quad p^* = \frac{M}{\alpha} \frac{\partial \varphi^*}{\partial x^*},$$

$$y^* = 0, \quad \frac{\partial \varphi^*}{\partial x^*} = 0;$$

$$y^* = \pi^+, 0 < x^* < l \quad \frac{\partial \varphi^*}{\partial y^*} = M \cdot \gamma(x^*) \frac{1}{\alpha};$$

1. $y^* = \pi^-, 0 < x^*; \quad y^* = \pi^+, l < x^* \quad \frac{\partial \varphi^*}{\partial x^*} = 0$ (10)
2. $y^* = \pi^-, l < x^*; \quad y^* = \pi^+, 0 < x^* \quad \frac{\partial \varphi^*}{\partial x^*} = 0$
3. $$y^* = \pi^-, 0 < x^* < s \quad \frac{\partial \varphi^*}{\partial x^*} = -\frac{\Delta P \alpha}{\rho_0 V_0 a}$$
$$y^* = \pi^+, l < x^* < s \quad \frac{\partial \varphi^*}{\partial x^*} = -\frac{\Delta P \alpha}{\rho_0 V_0 a}$$
$$y^* = \pi^{\pm}, s < x^* \quad \frac{\partial \varphi^*}{\partial x^*} = 0.$$

$$\sin\theta \approx tg\,\theta = \frac{dy}{dx}. \quad tg\,\theta = \frac{1}{\alpha} \frac{dy^*}{dx^*} = \frac{1}{\alpha} \gamma(x^*).$$

In successive derivations star in dimensionless value symbols will be omitted. The problem is reduced to developing analytical function in the domain $y > 0$ with a cut $y = \pi, x > 0$, satisfying boundary conditions (10). The solution will be developed in the form of a real part for the analytical function of a complex variable $\varphi(x, y) = \mathrm{Re}\,\Phi(z), \quad z = x + iy$. Thus development of the analytical function is reduced to Riemann – Hilbert problem. The latter for a special function type is reduced to Dirichlet problem. The solution for the Dirichlet problem is given by Schwarz integral. In case inclination angle is constant this integral can be taken in elementary functions. The

projections of forces are given by the following formulas:

$$X = \frac{\rho a^2 h M^2 \gamma_0^2 (\sqrt{u_0^+} - 1)^2}{2\alpha^2};$$

$$Y = -\frac{\rho a^2 h M^2 \gamma_0 (\sqrt{u_0^+} - 1)^2}{2\alpha}$$

- flow separation from the upper surface of the fragment, singularity at the front edge of the plate.

$$X = \frac{\rho a^2 h M^2 \gamma_0^2 (2\sqrt{u_0^+} - 3u_0^+ + u_0^{+2})}{\alpha^2 u_0^+};$$

$$Y = -\frac{\rho a^2 M^2 \gamma_0 (2\sqrt{u_0^+} - 3u_0^+ + u_0^{+2})}{\alpha u_0^+}$$

- flow separation from the upper surface of the fragment, singularity at the rear edge of the plate.

$$X = \frac{\rho a^2 h M^2 \gamma_0^2 (\sqrt{u_0^-} - 1)^2}{2\alpha^2};$$

$$Y = \frac{\rho a^2 h M^2 \gamma_0 (\sqrt{u_0^-} - 1)^2}{2\alpha}$$

- flow separation from the lower surface of the fragment, singularity at the front edge of the plate.

$$X = \frac{\rho a^2 h M^2 \gamma_0^2 (-2\sqrt{u_0^-} + 3u_0^- - u_0^{-2})}{\alpha^2 u_0^-};$$

$$Y = \frac{\rho a^2 M^2 \gamma_0 (-2\sqrt{u_0^-} + 3u_0^- - u_0^{-2})}{\alpha u_0^-}$$

- flow separation from the lower surface of the fragment, singularity at the rear edge of the plate.

The projection X represents the drag force, and projection Y – lift force, where $u_0^{\pm}$ are the roots of algebraic equation

$$l = u_0 - \ln|u_0| - 1.$$

Formulas below represent the solution for the case of closed cavity of final length, flow separation from the upper surface of the fragment, singularity at the front edge of the plate.

$$X = \frac{\rho a^2 h M^2 \gamma_0^2 (2\sqrt{u_0^+} - 3u_0^+ + u_0^{+2})}{\alpha^2 u_0^+} +$$

$$+ \frac{\rho a h M \gamma_0 \Delta P (u_0^+ + 1)}{2\rho_0 V_0 \pi} \ln \left| \frac{(1 + \sqrt{\frac{s_0^+ - u_0^+}{s_0^+ - 1}})(1 - \sqrt{\frac{s_0^- - u_0^+}{s_0^- - 1}})}{(1 - \sqrt{\frac{s_0^+ - u_0^+}{s_0^+ - 1}})(1 + \sqrt{\frac{s_0^- - u_0^+}{s_0^- - 1}})} \right| \frac{(2\sqrt{u_0^+} - 3u_0^+ + u_0^{+2})}{(u_0^+ - 1)^3} + \frac{M^2 \gamma_0^2}{\alpha^2} \frac{\Delta P h}{\pi} (u_0^+ - \ln u_0^+ - 1)$$

$$Y = -\frac{\rho a^2 h M^2 \gamma_0 (2\sqrt{u_0^+} - 3u_0^+ + u_0^{+2})}{\alpha u_0^+} -$$

$$- \frac{\rho a h M \alpha \Delta P (u_0^+ + 1)}{2\rho_0 V_0 \pi} \ln \left| \frac{(1 + \sqrt{\frac{s_0^+ - u_0^+}{s_0^+ - 1}})(1 - \sqrt{\frac{s_0^- - u_0^+}{s_0^- - 1}})}{(1 - \sqrt{\frac{s_0^+ - u_0^+}{s_0^+ - 1}})(1 + \sqrt{\frac{s_0^- - u_0^+}{s_0^- - 1}})} \right| \frac{(2\sqrt{u_0^+} - 3u_0^+ + u_0^{+2})}{(u_0^+ - 1)^3} - \frac{M^2 \gamma_0}{\alpha} \frac{\Delta P h}{\pi} (u_0^+ - \ln u_0^+ - 1)$$

Here $s_0^{\pm}$ are the roots of algebraic equation

$$s = s_0 - \ln|s_0| - 1.$$

The length of the cavity is determined from the condition of equality of the sum of upper and lower borders of the cavity vertical movements to vertical size of the cavity. In case of relatively small depth the following relation between the lengths of the fragment and cavity was obtained:

$$\frac{L}{2S} = \frac{e^{-2(\frac{\pi L}{\alpha h})}}{1 + e^{-2(\frac{\pi L}{\alpha h})} \cdot \frac{(\frac{2}{\alpha} - 1)\rho_0 V_0^2 \gamma_0 \pi}{\Delta P \alpha} \sqrt{\frac{\pi L}{\alpha h}}} \quad (11)$$

APPROXIMATION FORMULAS

Analysis of obtained results shows the asymptotic behavior of the forces depending on the ratio of fragment length, fluid layer thickness and pressure in the cavity.

In case fluid separation takes place from the upper side of the fragment two flow scenarios are possible having singularity on the front edge and on the rear edge. [14]

The front edge separation case has the following asymptotic solutions:

1) $h/L \to 0$: $X = \frac{\rho a^2 h M^2 \gamma_0^2}{2\alpha^2}(\sqrt{\frac{L\pi}{h\alpha}} - 1)^2$;

$Y = -\frac{\rho a^2 h M^2 \gamma_0}{2\alpha}(\sqrt{\frac{L\pi}{h\alpha}} - 1)^2$;

2) $h/L \to \infty$: $X = \frac{1}{2}\frac{\rho a^2 M^2 \gamma_0^2 \pi L}{\alpha^3}$;

$Y = -\frac{1}{2}\frac{\rho a^2 M^2 \gamma_0 \pi L}{\alpha^2}$.

As it is seen the above formulas turn to be quite simple for the limiting cases of very big or small depth, while for all the intermediate cases of interest they are rather complicated to be used directly. Due to that reason approximation formulas were developed.

Numerical simulations based on the obtained solution made it possible to develop approximation formulas for dimensionless forces depending on parameter $l = \frac{\pi L}{\alpha h}$:

$F_X = \frac{X \cdot \alpha^3}{\frac{1}{2}\rho V_0^2 \gamma_0^2 L} = \pi - \frac{\pi}{2} e^{-0,7l}$;

$F_Y = \frac{Y \cdot \alpha^2}{\frac{1}{2}\rho V_0^2 \gamma_0 L} = -\pi + \frac{\pi}{2} e^{-0,7l}$

This parameter characterizes both relative depth of fragment motion (depth as related to the size of a fragment) and its velocity as compared with wave propagation velocity in fluid. Parameter $l = \frac{\pi L}{\alpha h}$ increases on decreasing depth and increasing velocity (only subsonic case is regarded), and increases on decreasing velocity and increasing depth. The velocity dependence is essentially non-linear.

The rear edge separation case has the following asymptotic solutions:

1) $h/L \to 0$:

$X = \frac{\rho a^2 h M^2 \gamma_0^2}{\alpha^2}(2\sqrt{\frac{h\alpha}{L\pi}} - 3 + \frac{L\pi}{h\alpha})$;

$Y = -\frac{\rho a^2 h M^2 \gamma_0}{\alpha}(2\sqrt{\frac{h\alpha}{L\pi}} - 3 + \frac{L\pi}{h\alpha})$;

2) $h/L \to \infty$: $X = 3\frac{\rho a^2 M^2 \gamma_0^2 \pi L}{\alpha^3}$;

$Y = -3\frac{\rho a^2 M^2 \gamma_0 \pi L}{\alpha^2}$.

Approximation formulas for dimensionless forces depending from parameter $l = \frac{\pi L}{\alpha h}$ were developed:

$F_X = \frac{X \cdot \alpha^3}{\frac{1}{2}\rho V_0^2 \gamma_0^2 L} = 2\pi + \pi\left(1 - 0,4l^{0,4}\right)e^{-0,8l}$;

$F_Y = \frac{Y \cdot \alpha^2}{\frac{1}{2}\rho V_0^2 \gamma_0 L} = -2\pi - \pi\left(1 - 0,4l^{0,4}\right)e^{-0,8l}$

In case fluid separation takes place from the bottom of the fragment two flow scenarios are possible having singularity on the front edge and on the rear edge.

The front edge separation case has the following asymptotic solutions:

1) $h/L \to 0$: $X = \frac{\rho a^2 h M^2 \gamma_0^2}{2\alpha^2}$;

$Y = \frac{\rho a^2 h M^2 \gamma_0}{2\alpha}$;

2) $h/L \to \infty$: $X = \frac{\pi \rho a^2 M^2 \gamma_0^2 L}{4\alpha^3}$;

$Y = \frac{\pi \rho a^2 M^2 \gamma_0 L}{4\alpha^2}$.

Approximation formulas for dimensionless forces depending from parameter $l = \frac{\pi L}{\alpha h}$ were developed:

$F_X = \frac{X \cdot \alpha^3}{\frac{1}{2}\rho V_0^2 \gamma_0^2 L} = \frac{\pi}{2}\left(1 - 0,1l^{0,5}\right)e^{-0,7l}$;

$F_Y = \frac{Y \cdot \alpha^2}{\frac{1}{2}\rho V_0^2 \gamma_0 L} = \frac{\pi}{2}\left(1 - 0,1l^{0,5}\right)e^{-0,7l}$

The rear edge separation case has the following asymptotic solutions:

1) $h/L \to 0$:

$X = -\frac{2\rho a^2 h M^2 \gamma_0^2}{\alpha^2} e^{\frac{\pi L}{2\alpha h}}$; $Y = -\frac{2\rho a^2 h M^2 \gamma_0}{\alpha} e^{\frac{\pi L}{2\alpha h}}$

;

2) $h/L \to \infty$: $X = \frac{3}{2}\frac{\rho a^2 M^2 \gamma_0^2 \pi L}{\alpha^3}$;

$Y = \frac{3}{2}\frac{\rho a^2 M^2 \gamma_0 \pi L}{\alpha^2}$.

Approximation formulas for dimensionless forces depending from parameter $l = \frac{\pi L}{\alpha h}$ were developed:

$$F_X = \frac{X \cdot \alpha^3}{\frac{1}{2}\rho V_0^2 \gamma_0^2 L} = 2\pi + \pi\left(1 - 0,4 l^{0,4}\right) e^{-0,8l};$$

$$F_Y = \frac{Y \cdot \alpha^2}{\frac{1}{2}\rho V_0^2 \gamma_0 L} = 2\pi + \pi\left(1 - 0,4 l^{0,4}\right) e^{-0,8l}$$

Using the relation (11) the drag and lift forces in case of cavity formation may be estimated for relatively small depth.

$$X = \frac{\rho a^2 M^2 \gamma_0^2 L\pi}{\alpha^3} + \frac{\rho \gamma_0 \Delta P L^2 \pi}{2\rho_0 h \alpha^2}\left(\frac{2\pi L}{\alpha h} + \ln\left(1 + e^{-2\left(\frac{\pi L}{\alpha h}\right)} \cdot \frac{\left(\frac{2}{\alpha} - 1\right)\rho_0 V_0^2 \gamma_0 \pi}{\Delta P \alpha}\sqrt{\frac{\pi L}{\alpha h}}\right)\right) + \frac{M^2 \gamma_0^2 \Delta P L}{\alpha^3}$$

$$Y = -\frac{\rho a^2 M^2 \gamma_0 L\pi}{\alpha^2} - \frac{\rho \Delta P L^2 \pi}{2\rho_0 h \alpha}\left(\frac{2\pi L}{\alpha h} + \ln\left(1 + e^{-2\left(\frac{\pi L}{\alpha h}\right)} \cdot \frac{\left(\frac{2}{\alpha} - 1\right)\rho_0 V_0^2 \gamma_0 \pi}{\Delta P \alpha}\sqrt{\frac{\pi L}{\alpha h}}\right)\right) - \frac{M^2 \gamma_0 \Delta P L}{\alpha^2}$$

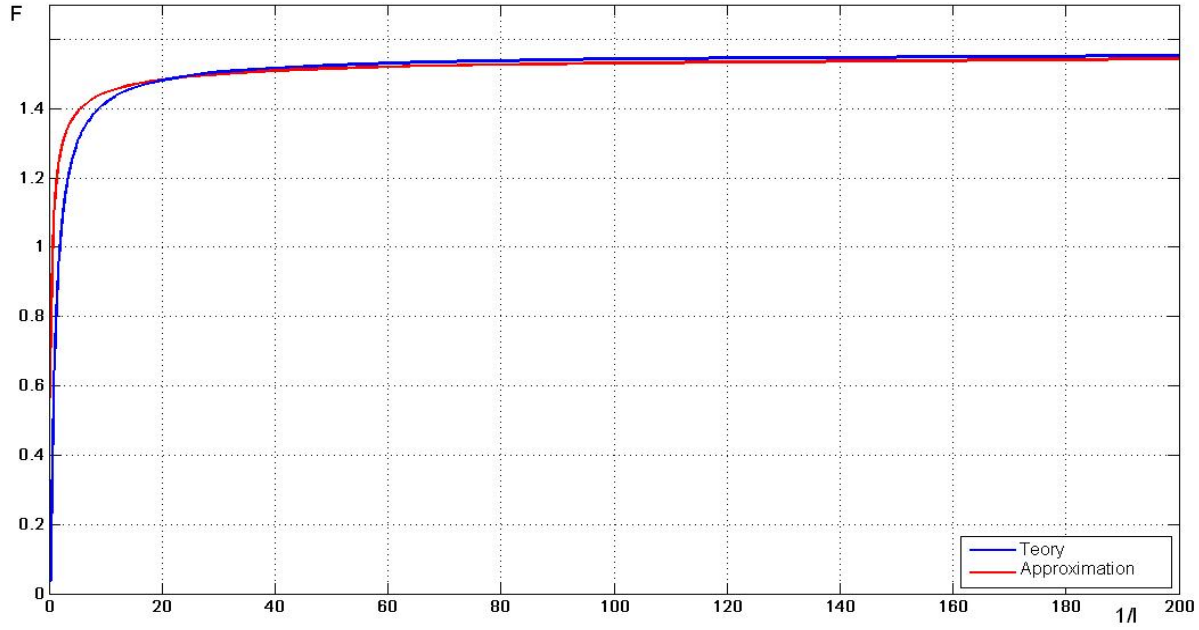

Fig.6. Relation between the force F_x and dimensionless parameter $1/l = (\alpha h)/(\pi L)$ obtained numerically and using approximation formula in case of separation from the bottom of the fragment having singularity on the front edge.

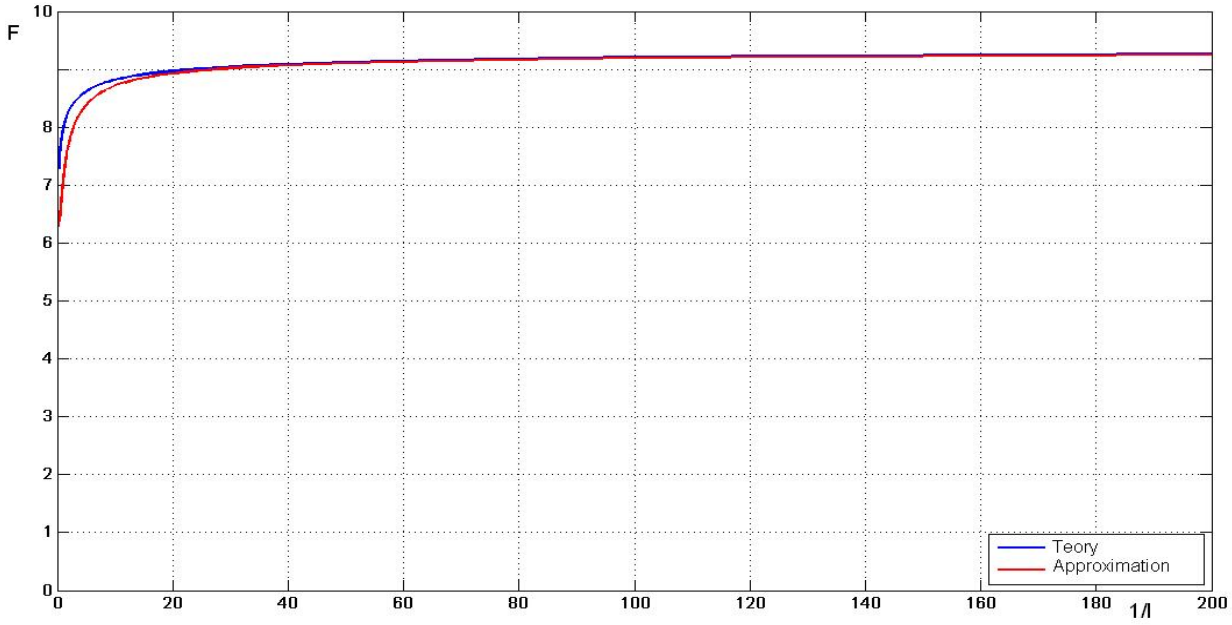

Fig.7. Relation between the force F_x and dimensionless parameter $1/l = (\alpha h)/(\pi L)$ obtained numerically and using approximation formula in case of separation from the upper side of the fragment having singularity on the rear edge.

Comparison of approximation formulas and exact solutions is provided in Figs. 6 and 7.
As it is seen from Figs. 6 and 7 the developed approximation formulas provide sufficient precision for a wide range of governing dimensionless parameter variation.

Thus, solution was obtained for a problem of fragment motion in compressible fluid at a final depth, constant velocity and inclination angle. Both cases of positive and negative inclination were regarded, which means flow separation from the upper side and bottom side of the fragment. Both cases of infinite cavity behind the fragment and final length cavity were regarded. For the case of final length cavity vapor pressure in it is less then the pressure on free surface.

The solution allows determining drag and lift forces in the limiting cases, the relation between the fragment length and the cavity length in the case of small depth. The forces increase when the pressure in the cavity decreases.

FRAGMENTS DECELERATION IN A FLUID-FILLED CONTAINMENT

Below estimates will be provided for fragment slowing down on penetrating containment partially filled with fluid, and for the dynamics of its energy conversion into the energy of expanding shock waves loading the containment from inside. At this stage of our study compressibility effects would play essential role in converting kinetic energy of a fragment into the energy of a blast wave expanding from the zone of energy release.
Formulas for resistance force acting on the plate moving in liquid parallel to free surface were used to simulate fragments deceleration. Analysis of formulas obtained in the previous section made it possible to develop the following simplified formula for resistance force:

$$F = \frac{1}{2}\rho V_\infty^2 C_d (1 - e^{-\frac{h}{L}})\pi r^2 . \qquad (12)$$

Integration of momentum equation for the fragment motion affected by the resistance force (25) yields

$$V = V_0 e^{-\frac{B}{m}x} \text{ ,where } B = \frac{1}{2}\rho C_d (1 - e^{-\frac{h}{L}})\pi r^2 \qquad (13)$$

The rate of energy release due to deceleration of the impactor in liquid filling containment is determined by formula:

$$\Theta = \frac{mV_0^2}{2} - \frac{mV_0^2}{2} e^{-\frac{B}{m}2x} = \frac{mV_0^2}{2}\left(1 - e^{-\frac{B}{m}2x}\right) \qquad (14)$$

Calculations were performed taking parameters corresponding to experiments [12] as an example. Drag coefficient was assumed to be $C_d = 1.68$.

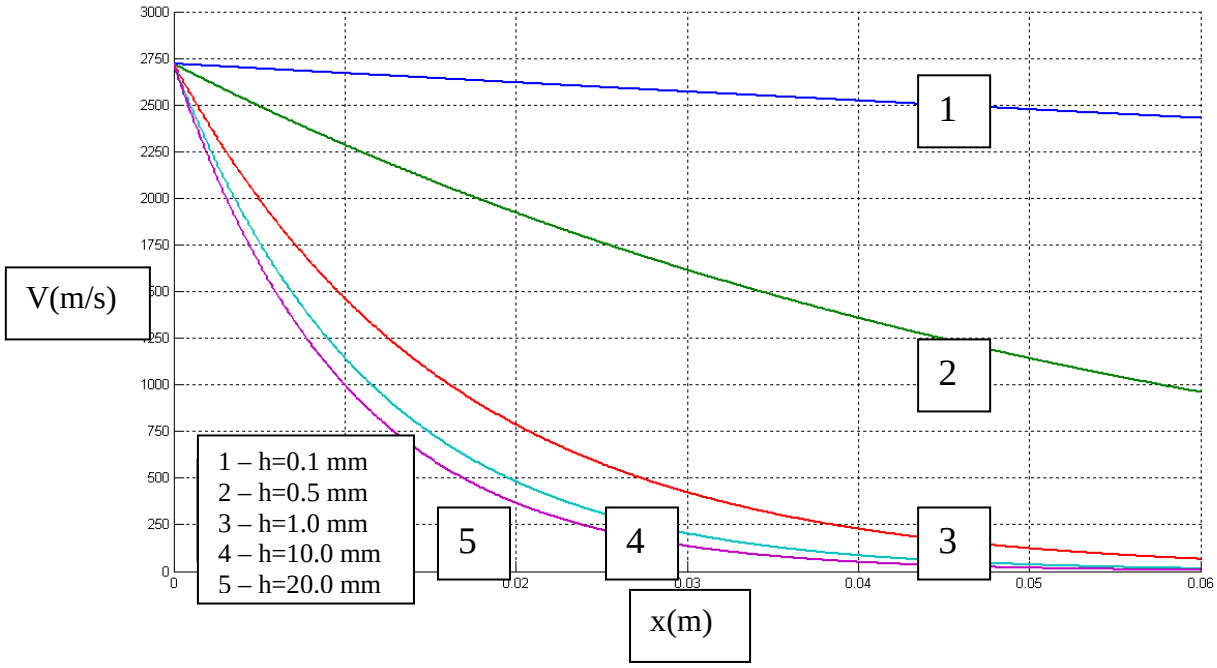

Fig. 8. Velocity(m/s) versus distance(m) for different depths of fragment $m = 0.335g$ motion under free surface.

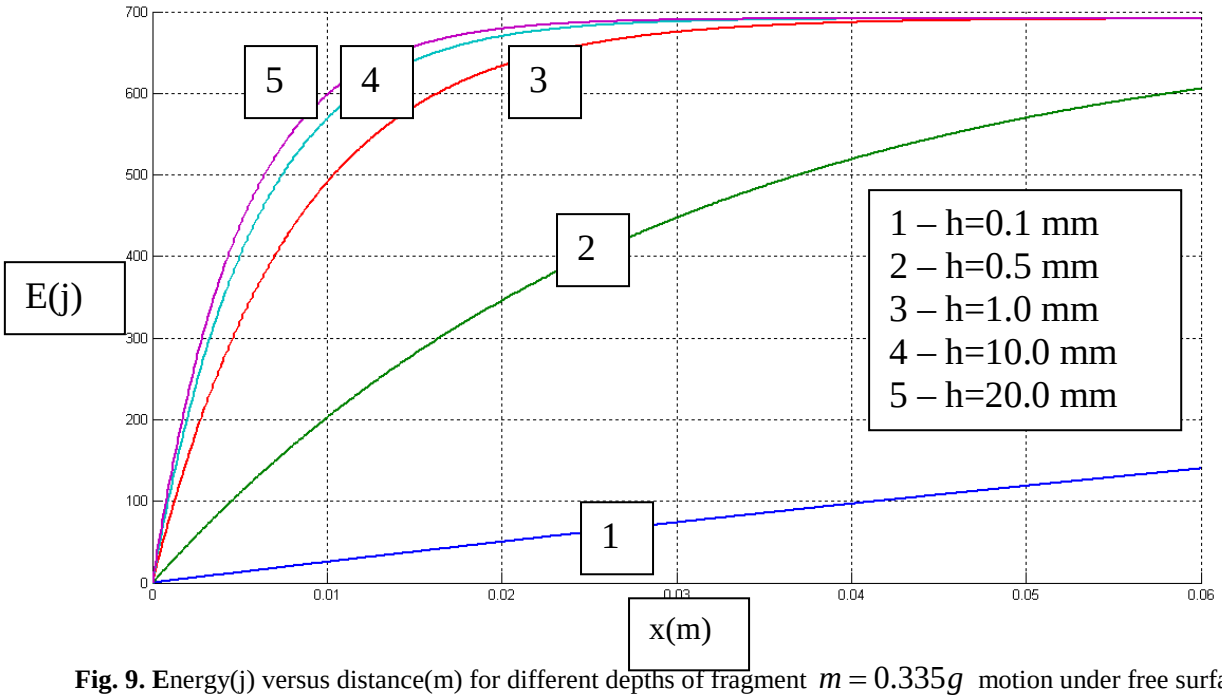

Fig. 9. Energy(j) versus distance(m) for different depths of fragment $m = 0.335g$ motion under free surface.

Fig. 8 illustrates the dependence of fragment velocity on distance for different depths of its motion under free surface. Initial fragment velocity was assumed 2720 m/s, fragment mass 0.335g. It is seen that for the small depth 0.1 mm (practically gliding along the surface) fragment's deceleration is negligibly small and its velocity, practically, does not change. The energy released to form shock wave internal loading of containment is negligible small as well (Fig. 9) However, 20 mm depth already brings to essential deceleration and absolute velocity loss takes place practically at a distance 60 mm. Fig. 9 illustrates the dependence of released energy versus distance for different depths of fragment motion. As seen from Fig.9 moving at a depth 20 mm brings to 95% energy release after fragment penetrates 15 mm, which should initiate shock wave most strongly affecting front wall. Thus on penetrating the containment deep under the

surface fragment should rather cause damage of the front wall, while penetrating the containment more close to free surface would bring to much smaller deceleration, most part of energy being released near the rear wall or preserved within the impactor. Under these conditions maximal damage could appear on the rear wall.

FRAGMENTATION ON FRONT WALL

In case velocity of impact and strength limit of impactor material are in combination resulting in fragmentation of a fragment and a part of the front wall a different flow scenario can take place. Small frgments partially penetrate inside the containment forming a cloud, and partially propagate in the opposite direction forming the so-called ejecta. Fig. 10 illustrates experimental (a) and theoretical (b) results on thin wall perforation and cloud formed in impact of a 5 mm particle at a velocity 5 km/s.

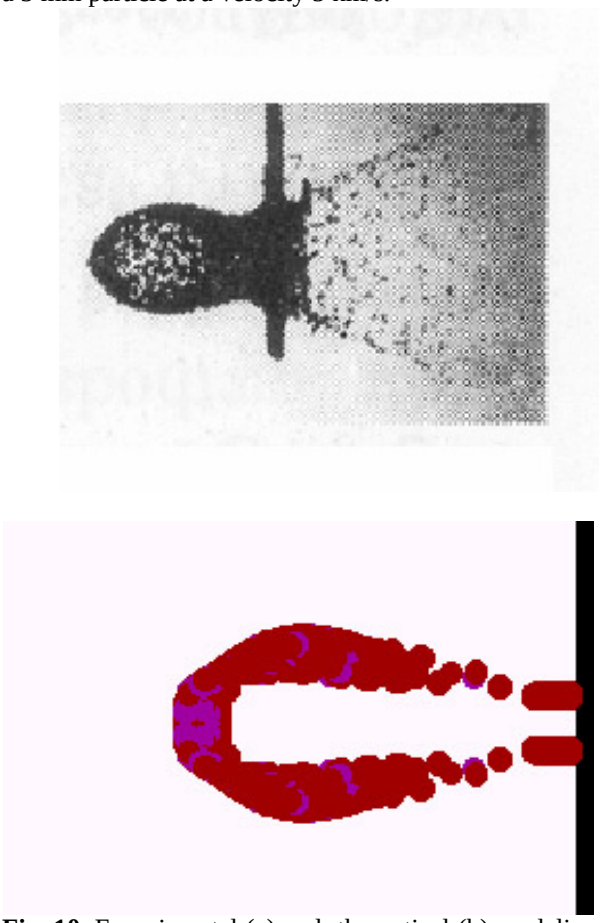

Fig. 10. Experimental (a) and theoretical (b) modeling of fragmentation in particle impact on metallic wall.

The cloud of small fragments decelerate much faster than a single fragment. Thus energy release will take place more close to the front wall. Thus, the investigated structure – fluid filled containments – could tern to be an effective protection in hypervelocity impact as well.

ANALYSIS OF RESULTS

It was demonstrated that on slowing down the fragment conversion of its kinetic energy into the internal energy of the surrounding gas (or fluid) takes place. The rapid increase of the density of energy in a small volume inside the containment gives birth to diverging blast waves inside the containment that reflects from the walls thus producing non-uniform loading.

The less is the fluid density, the slower is deceleration, and the weaker is the shock wave formed inside containment. Due to that reason increase of overall initial pressure brings to formation of stronger shock waves and increase of the damage level. Penetration of fragment deep below the liquid level also brings to its faster deceleration due to much higher density ratio as compared to deceleration in gas. However, overall drag coefficient is dependent on the depth of fragment motion below the liquid-gas interface, because gas is highly compressible as compared with liquid, which permits fluid separation from the fragment thus reducing the drag on approaching the free surface.

The partial filling of containment by fluid creates the conditions, under which maximal damages of a containment could evolve from the rear wall to the front wall, which was demonstrated both theoretically and experimentally.

CONCLUSIONS

Mathematical model for the fragment impact on a rather thin-walled containment, which could be filled in with gas, liquid, or both liquid and gas phases having a distinct phase interface was developed.

That creates an option for designing an effective shield for protecting different structures, especially orbital stations thus decreasing the hazardous consequences of Space debris particles impact.

ACKNOWLEDGEMENTS

The authors wish to acknowledge the support by Russian Foundation for Basic Research (Grant 12-08-00319).

REFERENCES

1. Smirnov N.N., (Ed.) *Space Debris Hazard Evaluation and Mitigation.* Taylor and Francis Publ., London, 2002, 208p.
2. Chobotov V.A. (Ed.). *Orbital Mechanics (2nd ed.).* AIAA Education Series, Washington, D.C., 1996.
3. Smirnov N.N. Evolution of Orbital Debris in Space. Advances in Mechanics, 2002. V.1, №2, pp. 37-104.
4. Silnikov M.V, Mikhailin A.I. Protection of wide-fragment aircraft against blast loads. Acta Astronautica (2014), 97 (1), 30-37.

5. Gelfand B.E., Silnikov M.V., Chernyshov M.V. On the efficiency of semi-closed blast inhibitors // Shock Waves. 2010. Vol. 20. No. 4. P. 317-321.
6. Smirnov, N.N., Kiselev, A.B., Nazarenko, A.I. Mathematical modeling of space debris evolution in the near Earth orbits 2002 Moscow University Mechanics Bulletin, Allerton Press. (*Vestnik Moskovskogo Universiteta. Ser. 1 Matematika Mekhanika)* (4), pp. 33-41
7. Smirnov, N.N., Nazarenko, A.I., Kiselev, A.B. Modelling of the space debris evolution based on continua mechanics 2001 *European Space Agency, (Special Publication) ESA SP* 1 (473), pp. 391-396.
8. Smirnov, N.N., Nikitin, V.F., Kiselev, A.B. Peculiarities of space debris production in different types of orbital breakups 1997 *European Space Agency, (Special Publication) ESA SP* (393), pp. 465-470.
9. Smirnov, N.N., Kiselev, A.B., Nikitin, V.F. Investigation of high-speed collisions of space debris particles with gas-filled shells 2003 Moscow University Mechanics Bulletin, Allerton Press. (*Vestnik Moskovskogo Universiteta. Ser. 1 Matematika Mekhanika*) (1), pp. 54-66
10. Smirnov, N.N., Kiselev, A.B., Kondrat'ev K.A. Zolkin S.N. Impact of debris particles on space structures modeling. Acta Astronautica 67 (2010), 333–343. doi: 10.1016/j.actaastro.2010.03.003
11. N.N.Smirnov, K.A.Kondratyev, Evaluation of craters formation in hypervelocity impact of debris particles on solid structures, Acta Astronautica 65 (2009), 1796–1803, doi: 10.1016/j.actaastro.2009.04.003
12. Pang Baojun, Zhang Wei, Luo Dekun and Zhang Zehua. Experimental investigation into water-filled pressurized vessels damaged by high-velocity projectile impact. Harbin Institute of Technology. *European Space Agency, (Special Publication) ESA SP* 2 (473), 2001, pp. 603-606.
13. Silnikov M.V., Chernyshov M.V., Uskov V.N. Two-dimensional over-expanded jet flow parameters in supersonic nozzle lip vicinity // Acta Astronautica. 2014. Vol. 97. Pp. 38-41.
14. Silnikov M.V., Chernyshov M.V., Uskov V.N. Analytical solutions for Prandtl-Meyer wave – oblique shock overtaking interaction // Acta Astronautica. 2014. Vol. 99. Pp. 175-183.
15. Smirnova M.N., Kondrat'ev K.A. Space debris fragments impact on multi-phase fluid filled containments // ActaAstronautica, 2012. – v. 79. – pp. 12-19.
16. M.N. Smirnova, A.V. Zvyaguin. Fluid flow interaction with an obstacle near free surface. Acta Astronautica 64 (2009) 288-294.
17. M.N. Smirnova, A.V. Zvyaguin. Different flow scenario for thin body subsonic motion in compressible fluid under free surface, Acta Astronautica 66 (2010), 434 -- 438, doi: 10.1016 /j.actaastro.2009.07.002